Orientation-dependent surface and step energies of Pb from first principles

Dengke Yu,[1] H. P. Bonzel,[2] and Matthias Scheffler[1]
[1]*Fritz-Haber-Institut der Max-Planck-Gesellschaft, Faradayweg 4-6, D-14195 Berlin-Dahlem, Germany*
[2]*Institut für Schichten und Grenzflächen, ISG 3, Forschungszentrum Jülich, D-52425 Jülich, Germany*
(Received 9 May 2006; revised manuscript received 13 July 2006; published 18 September 2006)

The orientation-dependent surface energies of 35 low-index and vicinal Pb surface orientations, located in the [001], [$\bar{1}$10], and [01$\bar{1}$] zones, have been calculated by density-functional theory within the local-density approximation. The highest surface energy anisotropies in these zones are at the (210), (110), and (311) directions. Surface relaxation decreases the surface energy anisotropy significantly. For misorientations smaller than 12° the (projected) surface energy in a given zone increases linearly with step density, while curvature is found at higher misorientations, indicative of repulsive step-step interactions. These results are fully consistent with the orientation-dependent surface energy predicted by the statistical mechanics of the terrace-step-kink model of vicinal surfaces. The step formation energies and surface and step relaxation energies are derived and analyzed. There is good agreement with available experimental data. The calculated surface energies in eV/atom correlate linearly with the number of broken surface bonds. Deviations from perfect linearity are found to be essential for a proper description of the equilibrium crystal shape of Pb.

DOI: 10.1103/PhysRevB.74.115408 PACS number(s): 68.35.Md, 61.50.Ah, 61.66.−f, 71.15.Mb

I. INTRODUCTION

Surface and step energies as well as step-step interaction energies of crystals are of fundamental importance in solid state physics and materials science: For example, they are needed to understand crystal growth, stability of thin films, and sintering of metal powders. The surface energy of a solid crystal depends on the crystallographic orientation, i.e., it is anisotropic. Most experimental data are unfortunately average values of an unknown range of orientations.[1,2] Only recently, it became possible to determine experimentally *absolute* values of surface free energies of a crystal for well-defined orientations, e.g., Pb.[3,4] The procedure involved fitting experimental equilibrium crystal and island shape data by Ising-type theoretical model equations[5] and using general thermodynamic considerations. Theoretical data, on the other hand, are available for many metals and semiconductors, with a large variation in magnitude due to the different approaches and approximations, utilizing empirical potentials,[6–8] tight-binding theory,[9,10] and density-functional theory (DFT).[11] It is equally important and interesting at this point to calculate systematically the orientation-dependent surface energy of a crystal, such as Pb, employing the accurate and reliable DFT method, and to compare the results directly with the experimental anisotropy obtained from equilibrium crystal shapes (ECSs).[12–15] A comparison of first-principles anisotropic surface energies with the generally accepted thermodynamic theory[16] is also of great interest, and should give a deeper, microscopic insight into the important physics of surface and step energies of materials.

There have been a number of DFT calculations of the low-index surface energies of Pb in the literature, showing a large scatter of results.[11,17–19] Previously we have rechecked the surface energies of Pb(111), Pb(100), and Pb(110) by DFT pseudopotential plane-wave calculations.[20,21] It was found that the calculated surface energies of Pb within the generalized gradient approximation (GGA) are about 30% lower than the experimental values, while results within the local-density approximation (LDA) are in good agreement with experiment. That the LDA yields more reliable surface energies than the GGA is probably due to a better error cancellation of the surface exchange and correlation energy within the LDA.[25] Surface relaxation is another important factor which typically decreases the surface energy by around 10%, depending on orientation. Numerical setups, such as the slab thickness, **k** mesh, and plane-wave cutoff, also affect the results.[21] In this study we extend our DFT calculations[20] of low-index surfaces of Pb to a systematic study of vicinal high-index orientations, suitable for a direct comparison with experimental investigations[3,4,26] and a detailed evaluation of step formation energies. The same data are used to estimate step-step interaction energies for the two principal zones of vicinal (111) surfaces. In the same context, relaxation energies of vicinal surfaces and steps are also evaluated and discussed. Finally, based on this extensive set of DFT surface energies for 35 different orientations of Pb, we check the validity of the broken surface bond rule for estimating surface energies of vicinal surfaces,[27] especially in the context of the equilibrium shape of small crystals at 0 K.[28]

II. DFT OF VICINAL SURFACE ENERGIES

The DFT total energy calculations were carried out for 32 vicinal Pb surfaces in their unrelaxed and relaxed configurations. The work essentially built on a previous extensive study of surface energies of low-index Pb surfaces.[21] The approach is based on *ab initio*, norm-conserving pseudopotentials.[20,22] Relativistic effects which may be important for Pb are accounted for by using a scalar-relativistic kinetic energy operator[23] which allows a proper description of the relativistic shifts of the valence levels while the spin-orbit coupling terms are averaged.[24] The exchange-correlation interaction is described within the local-density or the generalized gradient approximation.[22] The convergence of results was checked as a function of plane-wave cutoff, **k** mesh,

 ©2006 The American Physical Society

vacuum and slab thickness, and the effect of nonlinearity of the core-valence exchange-correlation interaction. Hence great care is taken to guarantee good numerical convergence.[21] We use a plane-wave cutoff of 14 Ry, Monkhorst-Pack **k** meshes equivalent or close to 24×24 for a Pb(100) surface, and slabs of 12 (111) layers in the terrace of the (111) vicinals, 14 (100) layers in the terrace of the (100) vicinals, and 18 (110) layers in the terrace of the (110) vicinals. The surface structures are fully relaxed, with a maximum force of 5–10 meV/Å. The average forces are one order of magnitude smaller. The error bar for the surface energies relative to each other is estimated to be smaller than ±0.1 meV/Å^2. Further calculational details may be found in Refs. 21 and 22.

Calculations were carried out for the [001] and [110] zones, bounded by the low-index (111), (100), and (110) surfaces. The results of surface energies for 32 high-index surfaces of Pb, together with the values of the low-index orientations published previously,[21] are listed in Table I. They are given in units of meV/Å^2 and also meV/atom which we will use later. The angle of orientation relative to the (111) surface, θ, is calculated for the [110] zone while for the [001] zone θ is equal to the sum of 35.264° and the relative angle to the (110) surface. The relative surface energy $\gamma(\theta)/\gamma_{(111)}$ versus orientation angle θ is plotted in Fig. 1 for both relaxed and unrelaxed surfaces. As expected, the minimum surface energy of 26.0 (27.5) meV/Å^2 is obtained at the close-packed (111) surface for relaxed (unrelaxed) structures. A secondary minimum is also found at (100). Maxima in each zone are observed at the (210), (110), and (311) orientations, which are all fully stepped structures. These open surfaces have the strongest surface relaxations due to the Smoluchowski charge smoothing effect.[29] Surface relaxation thus decreases the surface energy anisotropy significantly. The directions of maxima and minima of the theoretical anisotropy curve coincide well with experimental values obtained by evaluating the ECS of Pb at 323 and 473 K.[3,13] The degree of anisotropy for the relaxed surfaces at $T=0$ K is 25% and higher as expected, than the experimental values of 11% at 323 K (Ref. 3) and 6% at 473 K.[13]

The theoretical data in Fig. 1 show some important features which are not present or obvious in the experimental data. They may be characteristic of the temperature of 0 K. First, there is a small cusp at the (411) orientation. This surface is a special case because it exhibits two different steps per unit cell, with unequal step height and step separation. The same is true for the (551) surface. Vicinal surfaces of this kind appear to have relatively lower surface energies and thus higher stability than those with a single type of step.[28] This effect is more obvious for the unrelaxed surfaces. Note that the steps of all vicinal surfaces in this study are of monatomic height. Secondly, there are clear discontinuities in slope for the relaxed surfaces at the (320) and (110) orientations. The discontinuity at (320) is even present for the unrelaxed surface becoming enhanced through relaxation. Hence (320) represents a cusp orientation which actually leads to a facet on the $T=0$ K ECS.[28] On the other hand, at (110) there is a semicusp because the slope is near zero in the [110] zone but at a large positive value in the [001] zone, for both the relaxed surfaces. In other words, because of the twofold symmetry of this surface there is no (or a very shallow) cusp in the [110] zone but a pronounced cusp in the [001] zone. The corresponding facet on the ECS will be either a knife edge or of a highly anisotropic form.[28] This issue will be further discussed in the context of the step energies of vicinal (110) surfaces (see next section).

III. STEP FORMATION AND STEP-STEP INTERACTION ENERGIES

The increase in surface energy with step density for surfaces vicinal to a low-index cusp orientation is attributed to the formation energy of steps of monatomic height, f_1, and the step interaction energy f_3.[30] All three energies are temperature dependent but in this work we are considering the ground state situation at 0 K only. The step energy, which is equal to the energy per length divided by the step height, will be given in meV/Å^2. In general, the orientation dependence of the surface free energy is given by the following relationship derived in the framework of the terrace-step-kink model of vicinal surfaces:[31–33]

$$f(p) = f_0 + f_1 p + f_3 p^3, \tag{1}$$

where $f(p)=\gamma(\theta)/\cos(\theta)$ is the projected surface energy, and $p=\tan(\theta)$ the step density, f_0 the surface energy of the low-index orientation, and f_3 the step-step interaction energy due to elastic and electrostatic dipole-dipole interactions. Higher-order dipole-quadrupole interactions may also be present but their magnitude is generally negligible at large terrace width.[7,34] A quadratic p term is not taken into account.[31,32] Previous work on the shape exponent of vicinal surfaces of Pb has supported the universal exponent 3/2 which is consistent with the cubic p term.[35,36] The linear term in p is very important in Eq. (1) because it guarantees the formation of stable facets at low-index surfaces and low temperature on the ECS. In the limit of low step density the linear increase in $f(p)$ with misorientation $\tan(\theta)$ is therefore a characteristic feature of the orientation-dependent surface energy of vicinal surfaces. There is no simple rule up to which tilt angle the linearity should prevail, as long as the ratio f_3/f_1 is unknown. First-principles DFT calculations of the orientation-dependent surface energy should confirm the generic form of Eq. (1).

Based on the data set displayed in Fig. 1, theoretical step formation and step interaction energies can in principle be determined by fitting the calculated values of $f(\theta)$ versus $\tan(\theta)$ by Eq. (1). This is illustrated in Figs. 2(a) and 2(b) for relaxed Pb vicinal surfaces in the $[01\bar{1}]$ and $[\bar{1}10]$ zones over a range of orientations from zero to about 30° relative to (111). There is a nearly perfect linear behavior up to about $\tan(\theta)=0.22$, or $\theta=12°$. The step configurations of surfaces vicinal to (111) in these two zones are inequivalent because their ledge structure is (100) and (111) for $[01\bar{1}]$ and $[\bar{1}10]$ zones, respectively. These steps are commonly denoted as A and B steps. The straight lines in Figs. 2(a) and 2(b) yield different step formation energies of 15.8 and 13.9 meV/Å^2 for relaxed A and B steps, respectively, corresponding to a step energy ratio of 0.88. The two different energies reflect

TABLE I. Calculated DFT step formation energies of well-defined low- and high-index vicinal surface orientations of Pb for relaxed and unrelaxed surfaces. Values are given in meV/Å^2 as well as eV/surface atom. To convert one into the other, the area per unit cell and the number of broken surface bonds per unit cell are needed. The relative angle θ is used to display $\gamma(\theta)$ versus θ for both $\langle 001\rangle$ and $\langle 110\rangle$ zones.

Surface orientation (hkl)	Relative angle θ (deg)	Area of unit cell (Å^2)	Number of broken bonds	$\gamma(\theta)_{rel}$ (meV/Å^2)	$F(hkl)_{rel}$ (eV/atom)	$\gamma(\theta)_{unrel}$ (meV/Å^2)	$F(hkl)_{unrel}$ (eV/atom)
(100)	54.74	12.25	4	29.91	0.3664	32.05	0.3926
(15 1 1)	49.354	92.29	31	30.47	2.8122	33.13	3.0579
(11 1 1)	47.414	67.94	23	30.68	2.0843	33.47	2.2740
(911)	45.81	55.81	19	30.84	1.7209	33.75	1.8833
(711)	43.32	43.75	15	31.07	1.3591	34.07	1.4902
(511)	38.95	31.83	11	31.17	0.9920	34.43	1.0960
(411)	35.27	51.98	18	31.08	1.6154	34.13	1.7739
(311)	29.496	20.32	7	31.17	0.6332	34.88	0.7086
(211)	19.471	30.01	10	29.70	0.8913	32.91	0.9876
(533)	14.42	40.17	13	29.23	1.1740	31.96	1.2836
(322)	11.422	50.51	16	28.57	1.4432	31.15	1.5737
(755)	9.446	60.95	19	28.20	1.7186	30.62	1.8664
(433)	8.05	71.44	22	27.95	1.9966	30.23	2.1594
(544)	6.208	92.50	28	27.51	2.5444	29.62	2.7398
(655)	5.051	113.61	34	27.25	3.0957	29.25	3.3232
(111)	0	10.61	3	25.97	0.2756	27.53	0.2921
(665)	4.755	120.66	36	26.99	3.2566	29.07	3.5076
(554)	5.768	99.53	30	27.20	2.7068	29.39	2.9249
(443)	7.326	78.45	24	27.51	2.1581	29.85	2.3419
(332)	10.025	57.46	18	27.99	1.6086	30.63	1.7598
(553)	12.275	47.05	15	28.32	1.3327	31.16	1.4661
(221)	15.793	36.75	12	28.77	1.0575	31.92	1.1731
(331)	22	26.70	9	29.67	0.7922	33.04	0.8822
(551)	27.215	43.75	15	30.24	1.3228	33.23	1.4536
(110)	35.264	17.24	6	30.40	0.5240	35.03	0.6037
(650)	40.458	95.69	34	30.93	2.9594	35.85	3.4306
(540)	41.6	78.45	28	31.02	2.4332	36.01	2.8245
(430)	43.39	61.26	22	31.24	1.9136	36.22	2.2184
(320)	46.3	44.17	16	31.27	1.3815	36.33	1.6047
(210)	53.695	27.40	10	32.37	0.8867	37.36	1.0235
(310)	61.825	38.74	14	31.92	1.2365	36.31	1.4066
(410)	66.224	50.51	18	31.68	1.6004	35.60	1.7983
(510)	68.95	62.47	22	31.52	1.9692	35.13	2.1944
(710)	72.13	86.63	30	31.17	2.7001	34.40	2.9803
(910)	73.92	110.94	38	30.94	3.4329	33.96	3.7671

the structural difference of the two kinds of steps. Thus the threefold symmetry of (111) facets on the experimental[37,38] Pb ECS is confirmed by our first-principles results. The step energies of unrelaxed vicinal Pb(111) surfaces are much higher, namely, 21.3 and 20.0 meV/Å^2, respectively (ratio 0.94).

The step energy of vicinal Pb(100) surfaces in the [110] zone was evaluated in the same fashion, such as seen in Fig. 2(c), and yielded 8.9 and 13.3 meV/Å^2 for relaxed and unrelaxed surfaces, implying a step relaxation energy of 4.4 meV/Å^2. Although the ledge of these steps on (100) has the same microstructure as the B step of the vicinal (111) surface, the energy for creating a step on a close-packed (111) surface is obviously higher than on a less dense (100) surface. By contrast, the formation energy of a fully kinked step, formed by tilting the (100) surface in the [001] zone, is considerably higher at 11.2 (18.7) meV/Å^2 for the relaxed (unrelaxed) surface [Fig. 2(c)]. The step direction is [100] and the step is called a C step. The step energy ratio C/B for relaxed surfaces at the vicinal (100) orientation is 1.26. A

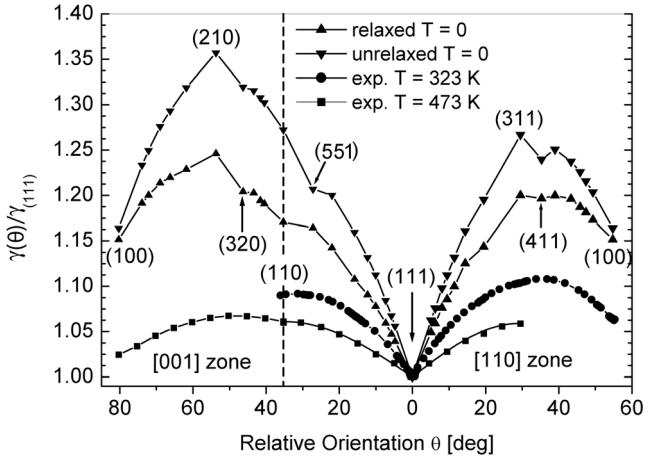

FIG. 1. Plot of $\gamma(\theta)/\gamma_{(111)}$ versus θ in the $\langle 001\rangle$ and $\langle 110\rangle$ zones for relaxed and unrelaxed Pb surfaces, respectively. Maxima in each zone are located at (210), (110), and (311). Real cusps exist at (111), (100), and (320) while a semicusp is noticed at the (110) orientation for relaxed surfaces. There are also local minima at (411) and (551) which are dual-step structures (see text). Experimental data taken at 323 K (Ref. 3) and 473 K (Ref. 13) are shown for comparison.

simple two-dimensional Wulff construction shows that the equilibrium shape of a (100) facet at 0 K is an irregular octagon with a step length ratio of $l_B/l_C=5.1$.

The evaluation of a step energy of vicinal (110) surfaces is possible only in the [001] zone because at (110) there is the already mentioned semicusp (compare the discussion of Fig. 1). The energy of the C-type step in this case is 5.9 and 8.5 meV/Å^2 for relaxed and unrelaxed surfaces, respectively. In the [110] zone there is practically no visible cusp at (110) in Fig. 1, implying a very low or zero step formation energy. The magnitude of this step energy (B type), however, has been estimated[28] from the theoretical ECS of relaxed Pb as 0.3 meV/Å^2. The step energy ratio B/C would then be about 0.05 which corresponds to a (110) facet, which exhibits a highly anisotropic shape at 0 K.

Returning to Fig. 2 we evaluate the small positive curvature in $f(\theta)$ versus $\tan(\theta)$, which indicates an overall repulsive step interaction for Pb vicinal surfaces at 0 K. At large terrace width, this repulsive interaction is very weak but at step densities larger than 0.2 it becomes obvious. For the relaxed Pb(111) vicinal surfaces the results are consistent with step interaction energies of the order of 4–5 meV/Å^2, estimated from the $f(\theta)$ versus $\tan(\theta)$ data of Figs. 2(a) and 2(b) for the range of $\tan(\theta)$ less than 0.5. At this point we wish to stress that these step interaction energies are course estimates because it is not known whether the strict form of Eq. (1) still holds at such high step densities. This interaction originates predominantly from the elastic force field of steps. By comparison, the electrostatic dipole-dipole interaction is estimated from calculated work function changes of stepped surfaces and was found to be smaller than 0.01 meV/Å^2. The theoretical total dipole-dipole step interaction energies (elastic and electrostatic) are smaller than the corresponding experimentally determined values of 8–11 meV/Å^2,[24,36] which may be a consequence of fitting our data by Eq. (1) outside the range of validity of this equation. The theoretical

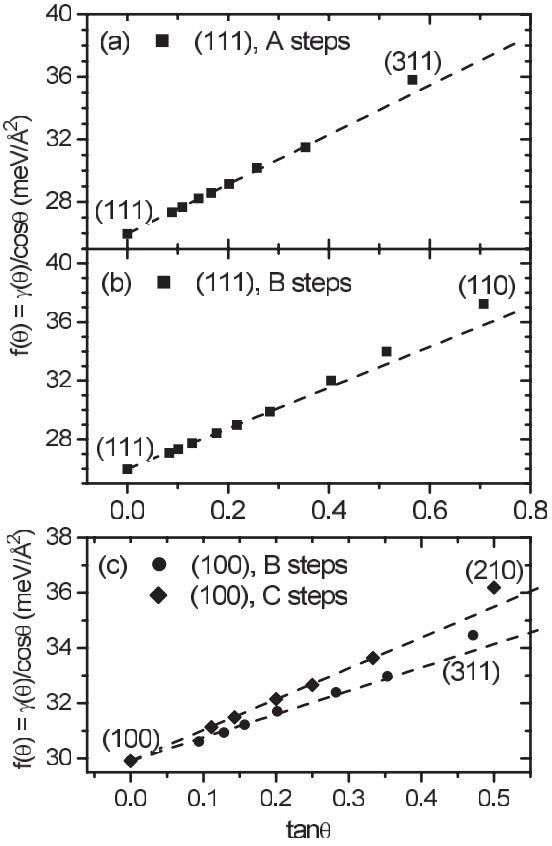

FIG. 2. Plot of $f(\theta)$ versus $\tan(\theta)$ for relaxed surfaces in the (a) $[01\bar{1}]$ and (b) $[\bar{1}10]$ zones, representing (111) vicinal A and B steps, and (c) the $[01\bar{1}]$ and [001] zones, representing the (100) vicinal B and C steps, respectively. The lines are linear fits to points up to $\tan(\theta)=0.22$. Points deviating from the lines at higher misorientation angles indicate positive curvature due to repulsive step-step interaction.

ratio of step interaction to step energy for (111) vicinal surfaces is about 1/3.

IV. RELAXATION ENERGIES OF VICINAL SURFACES AND STEPS

The differences in calculated surface and step formation energies for relaxed and unrelaxed surfaces allow the determination of corresponding relaxation energies. Based on Eq. (1), we define the surface relaxation energy of the vicinal surfaces as $\Delta f_{rel}(p)=f_{unrel}(p)-f_{rel}(p)=\Delta f_{rel}(0)+h[\Delta f_1(p)/d]$ (neglecting step-step interaction at low step densities), where h is the monatomic step height, d the terrace width, and $\Delta f_1(p)$ the step relaxation energy. This relationship holds for small tilt angles where the linear behavior of $f(\theta)$ versus $\tan(\theta)$ is valid. The surface relaxation energy of vicinal surfaces decreases with increasing terrace width (Fig. 3) and approaches asymptotically the value of the (111) terrace. The solid curves are calculated using a *constant* step relaxation energy. Hence, the surface relaxation energy of vicinal surfaces in this angular range is governed by a constant step relaxation energy.

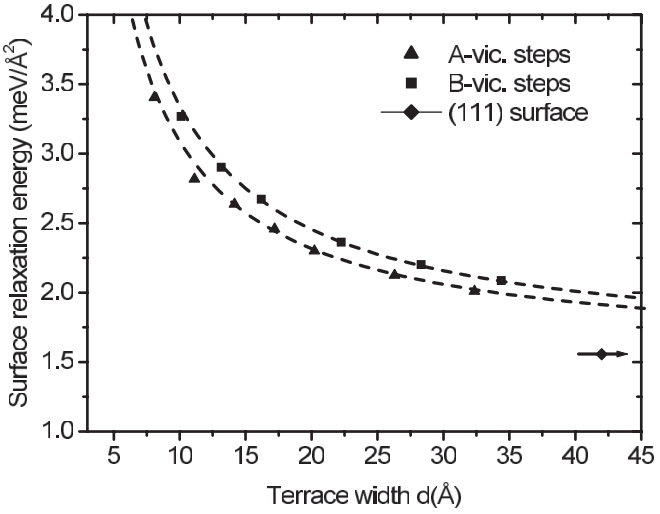

FIG. 3. Surface relaxation energies of Pb(111) vicinal orientations versus terrace width d in the $[01\bar{1}]$ and $[\bar{1}10]$ zones. Curves are calculated according to a $1/d$ dependence of the surface relaxation energy. The surface relaxation energy of the low-index Pb(111) is 1.56 meV/Å^2.

The step relaxation energy $\Delta f_1(p)$, calculated as the difference $[\Delta f_{rel}(p) - \Delta f_{rel}(0)]/\tan(\theta)$, is plotted in Fig. 4 versus step density for (111) vicinal A and B steps. In a range of tilt angles where the linearity of $f(\theta)$ versus $\tan(\theta)$ holds, the relaxation energies of A and B steps are indeed nearly constant at about 5 and 6 meV/Å^2, respectively. The (411) and (551) orientations are special cases because they exhibit two different types of steps per unit cell, with slightly different step heights and step separation. These surfaces deviate markedly from the behavior of surfaces with only one kind of monatomic step. They show lower relaxation energies, which is consistent with the local minima in the orientation-dependent surface energy plot in Fig. 1. There the minima at (411) and (551) are more pronounced for the unrelaxed surfaces and become shallower with relaxation.

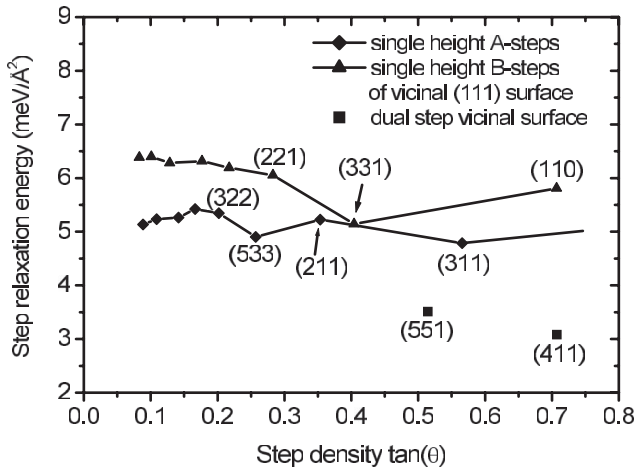

FIG. 4. Step relaxation energies of A and B steps of vicinal Pb(111) surfaces versus step density. Note the oscillation of the step relaxation energy at large tilt angle. Also note that the dual step structures (551) and (411) have much lower step relaxation energy.

V. DISCUSSION OF STEP FORMATION ENERGIES

The theoretical surface and step energies of (111), (100), and (110) vicinal surfaces in the [110] and [100] zones allow us to calculate the ratios of step to surface energy, which are structure specific. These are 0.60 and 0.51 for A and B steps on (111), 0.25 and 0.37 for B and C steps on (100), and 0.19 for the C step on (110). We can check whether these ratios are reasonable, by referring to a simple broken bond counting scheme[39,40] (compare Sec. VI), which produces the ratios in the same sequence as 0.67, 0.67, 0.25, 0.5, and 0.2, respectively.[41,42] There is relatively close agreement in the two sets of numbers, although DFT yields lower values for (111) and (100) in the [100] zone. For (110) in the [110] zone broken bond counting predicts zero for the ratio, while we estimate 0.01 utilizing data derived from the ECS which was constructed from the DFT results of Fig. 1.[28]

The comparison of the evaluated theoretical energies of A and B steps vicinal to Pb(111) with the corresponding experimental values[26] of 12.8 and 11.6 meV/Å^2 shows that the latter are lower by about 17–20 %. There is good agreement in the step energy ratio $f_{1B}(0)/f_{1A}(0)$ at 0 K, which is 0.91 experimentally and 0.88 theoretically. The experimentally determined ratios of step energy (at $T=0$ K) over Pb(111) surface energy (at finite T), $f_1(0)/f_0(T)$, are 0.47 and 0.42 for A and B steps, respectively.[3] They are considerably lower than the theoretical ratios. If we assume that the surface energy of Pb(111) does not vary significantly with temperature, it follows that theory predicts the facet radii to be larger than found experimentally. The deviation is about 18–22 %, which may still be reasonable in view of a number of error sources, especially in experiment.

On the other hand, the current theoretical step energies of Pb(111) are about 6 meV/Å^2 or at least 60% higher than the previously published DFT results within the GGA.[18] As noted earlier, we believe that LDA surface energies are more accurate than those obtained by the GGA. Indeed, the LDA results of surface energies for low-index orientations closely agree with experiment,[21] and the same is true for the high-index orientations. Hence step formation energies derived from the LDA theoretical surface energies are also believed to be more reliable. The main reason for the 17–20 % discrepancy with the experimental data can be traced to the scatter in the primary shape anisotropies of two-dimensional Pb(111) islands and facets[26,38] which were evaluated by fitting to theoretical Ising theory-type expressions.[5] The fit parameters were step formation energy (at 0 K) and kink formation energy, both for a particular step type. The relatively large scatter in data allows for a range of fit parameters. Although the originally quoted values of step and kink energies for Pb(111) A and B steps were obtained by a "best fit" procedure, other values, such as those found here from theoretical surface energies, also fit the same data reasonably well.[43] As a consequence, one would expect to find higher kink formation energies than those based on experiment. At this point it would be desirable to complement the current results for surface and step energies with additional calculations of kink energies by DFT using the LDA.

VI. THE BROKEN SURFACE BOND RULE

It is of general interest to conclude the presentation of our orientation-dependent surface energy data of Pb with an

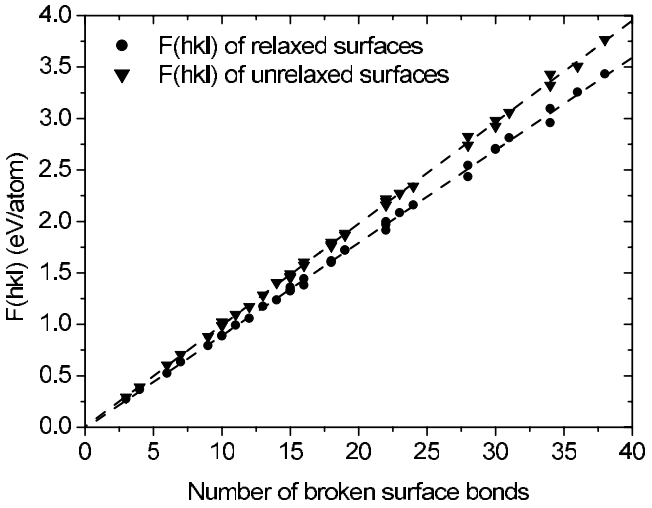

FIG. 5. Plot of theoretical surface energy $F(hkl)$ in eV per surface atom versus number of surface bonds which are broken in forming an (hkl) surface. DFT results are shown for unrelaxed and relaxed surfaces of Pb. The data are best fit by straight lines.

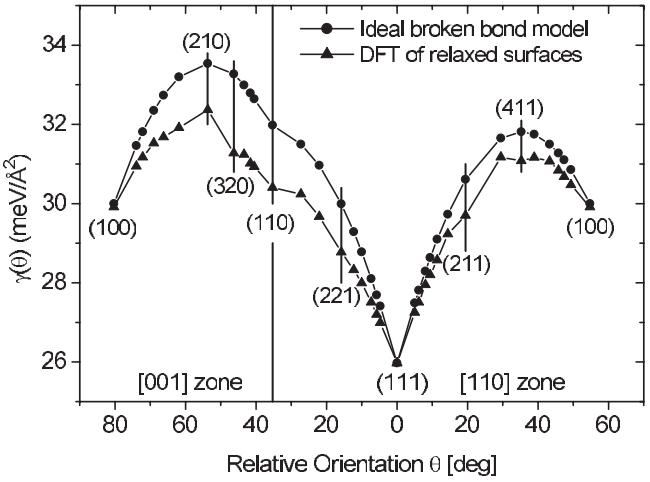

FIG. 6. Comparison of calculated $\gamma(\theta)$ versus θ functions in the $\langle 001\rangle$ and $\langle 110\rangle$ zones for the ideal broken surface bond model and the full DFT results for relaxed Pb surfaces. The two data sets are matched at the (111) orientation. Note the local changes in slope for the DFT data at the indicated vicinal orientations.

analysis which has been proposed by Galanakis *et al.*[17,27] These authors found an almost perfect linear correlation of computed surface energies, given in units of eV per surface atom, with the number of broken surface bonds (per unit cell). This correlation has recently also been demonstrated for Cu where surface energies of low-index and vicinal orientations have been computed by first principles.[44] Although the idea that the anisotropy of surface energies should scale with the number of broken surface bonds is not new,[45–47] it is rather surprising that theoretical values obtained by first principles seem to support this simple rule.[39,40] For surface energies, calculated for low-index and many high-index orientations of the same fcc metal, they yield a nearly perfect linear correlation.[44] Deviations from linearity are reported to be about 3–5 % for Cu. To check the broken surface bond rule for Pb, we converted our computed surface energies to units of eV per surface atom, according to $F(hkl)=\gamma(\theta)A(hkl)$, and plotted the results in Fig. 5 versus the number of broken surface bonds for all 35 unrelaxed and relaxed surfaces. $A(hkl)$ is the area per unit cell of the (hkl) surface. The number of broken surface bonds is formally defined by $N_{bb}(hkl)=2\alpha h+k$, where $\alpha=1$ for h,k odd and $\alpha=2$ for h and/or k even. Both quantities, $A(hkl)$ and the number of bonds per unit cell, $N_{bb}(hkl)$, are also listed in Table I. The data fall indeed on nearly perfect straight lines, with some points deviating slightly. The average energy per broken bond is about 10% higher for the unrelaxed surfaces.

Hence the current results for Pb are consistent with previous studies based on first-principles theory. They support the broken surface bond rule and as such indicate self-consistency of the theoretical anisotropic surface energy values. However, a closer analysis of the same data reveals some important details. Those surface orientations for which deviations from a perfect straight line are observed, are the ones where facets form on the equilibrium crystal shape.[28] These facets are not present on the ECS when an *exact* linearity of the surface energy $F(hkl)$ versus the number of broken surface bonds is assumed. This can best be seen in the corresponding function $\gamma(\theta)$ versus relative orientation θ in Fig. 6 which has no singularities except at the low-index orientations (111), (100), and (110), the latter only in the [001] zone; it is therefore markedly different from the theoretical DFT result in Fig. 1. A direct comparison of both functions for relaxed Pb surfaces is shown in Fig. 6.

Both functions $\gamma(\theta)$ were matched at the (111) orientation by setting the proportionality constant of $F(hkl)$ versus the number of broken surface bonds equal to $\gamma(111)A(111)$. We note in Fig. 6 that both data sets still agree closely at (100) but higher surface energies are observed for all other orientations. More importantly, nonsystematic large deviations are noted for the orientations (320), (110), (221), (211), and (411). These differences between the two surface energy functions have rather important consequences. First, step energies evaluated from the initial slopes of $d\gamma(\theta)/d\theta$ at low-index orientations are larger for the ideal broken bond function than for the exact DFT function. Second, the observed singularities (slope discontinuities) on the exact DFT $\gamma(\theta)$ function are associated with facets on the ECS except the (411).[28] This can be shown by performing a Wulff construction on the complete $\gamma(\theta)$ function in polar coordinates to obtain the ECS.[28] No such facets are obtained for the ideal broken surface bond function. Third, step-step interaction energies, which are related to the curvature of $\gamma(\theta)$, are also expected to be different for the two functions in Fig. 6. In summary, the broken surface bond rule may serve to estimate the surface energy of a high-index surface but it is a poor approximation when it comes to evaluating quantitative secondary energetic surface data and/or obtaining a realistic ECS. From a physics point of view, such a difference is expected because surface relaxation and surface charge smoothing[29] are neglected in the ideal broken surface bond model.[39,40] Higher-order atomic interactions have to be included in calculating surface properties of metals.[48] These interactions are responsible for subtle differences in surface

energies which then yield a realistic description of the anisotropy and the proper ECS at $T=0$ K.[28] In this sense there is a similarity between the $\gamma(\theta)$ function calculated for the ideal broken surface bond function and the DFT results computed for unrelaxed Pb surfaces because *both* do not give rise to extra facets on the ECS other than the low-index facets (111) and (100) as well as a knife-edge (110) facet.[28]

VII. SUMMARY AND CONCLUSIONS

In summary, an extensive set of first-principles DFT surface energy data of low-index and vicinal Pb surfaces has been obtained which allows the evaluation of step formation energies of vicinal (111), (100), and (110) surfaces. The (projected) surface energy of vicinal orientations increases linearly with step density over a range of about 10°–12° misorientation for all studied zones. A direct comparison of theoretical and experimental inequivalent *A* and *B* step energies of vicinal Pb(111) surfaces shows reasonable agreement, especially in the ratio $f_{1B}(0)/f_{1A}(0)$. Step relaxation energies as a function of step density are nearly constant at small tilt angles. Dual-step structures exhibit a much lower step relaxation energy. The ratios of step to surface energies are clearly structure specific. Step-step interactions are weakly repulsive due to elastic interactions. The calculated surface energies in eV/atom depend to a first order linearly on the number of broken surface bonds. An exact linear dependence, however, does not lead to all of the expected facets on the equilibrium crystal shape nor will it yield the proper step and step-step interaction energies.

[1] W. R. Tyson and W. A. Miller, Surf. Sci. **62**, 267 (1977).
[2] V. K. Kumikov and K. B. Khokonov, J. Appl. Phys. **54**, 1346 (1983).
[3] C. Bombis, A. Emundts, M. Nowicki, and H. P. Bonzel, Surf. Sci. **511**, 83 (2002).
[4] H. P. Bonzel, Phys. Rep. **385**, 1 (2003).
[5] N. Akutsu and Y. Akutsu, J. Phys.: Condens. Matter **11**, 6635 (1999).
[6] S. M. Foiles, M. I. Baskes, and M. S. Daw, Phys. Rev. B **33**, 7983 (1986).
[7] R. Najafabadi and D. J. Srolovitz, Surf. Sci. **317**, 221 (1994).
[8] J. W. M. Frenken and P. Stoltze, Phys. Rev. Lett. **82**, 3500 (1999).
[9] S. Papadia, M. C. Desjonquères, and D. Spanjaard, Phys. Rev. B **53**, 4083 (1996).
[10] F. Raouafi, C. Barreteau, M. C. Desjonquères, and D. Spanjaard, Surf. Sci. **482-485**, 1413 (2001).
[11] L. Vitos, A. V. Ruban, H. L. Skriver, and J. Kollár, Surf. Sci. **411**, 186 (1998).
[12] J. C. Heyraud and J. J. Métois, J. Cryst. Growth **50**, 571 (1980).
[13] J. C. Heyraud and J. J. Métois, Surf. Sci. **128**, 334 (1998).
[14] J. J. Métois and J. C. Heyraud, Surf. Sci. **180**, 647 (1987).
[15] Z. Wang and P. Wynblatt, Surf. Sci. **398**, 259 (1998).
[16] C. Herring, in *Structure and Properties of Solid Surfaces*, edited by E. Gomer and C. C. Smith (University of Chicago Press, Chicago, 1952), p. 5.
[17] I. Galanakis, N. Papanikolaou, and P. H. Dederichs, Surf. Sci. **511**, 1 (2002).
[18] P. J. Feibelman, Phys. Rev. B **62**, 17020 (2000); Phys. Rev. B **65**, 129902(E) (2002).
[19] C. M. Wei and M. Y. Chou, Phys. Rev. B **66**, 233408 (2002).
[20] M. Bockstedte, A. Kley, J. Neugebauer, and M. Scheffler, Comput. Phys. Commun. **107**, 187 (1997).
[21] D. Yu and M. Scheffler, Phys. Rev. B **70**, 155417 (2004).
[22] M. Fuchs and M. Scheffler, Comput. Phys. Commun. **119**, 67 (1999).
[23] D. D. Koelling and B. N. Harmon, J. Phys. C **10**, 3107 (1977).
[24] L. A. Hemstreet, C. Y. Fong, and J. S. Nelson, Phys. Rev. B **47**, 4238 (1993).
[25] V. N. Staroverov, G. E. Scuseria, J. Tao, and J. P. Perdew, Phys. Rev. B **69**, 075102 (2004).
[26] M. Nowicki, C. Bombis, A. Emundts, and H. P. Bonzel, Phys. Rev. B **67**, 075405 (2003).
[27] I. Galanakis, G. Bihlmayer, V. Bellini, N. Papanikolaou, R. Zeller, S. Blügel, and P. H. Dederichs, Europhys. Lett. **58**, 751 (2002).
[28] D. K. Yu, H. P. Bonzel, and M. Scheffler, New J. Phys. **8**, 65 (2006).
[29] R. Smoluchowski, Phys. Rev. **60**, 661 (1941).
[30] W. W. Mullins, in *Metal Surfaces: Structure, Energetics and Kinetics*, edited by W. D. Robertson and N. A. Gjostein (ASM, Metals Park, OH, 1963), pp. 17–66.
[31] E. F. Gruber and W. W. Mullins, J. Phys. Chem. Solids **28**, 875 (1967).
[32] C. Jayaprakash, C. Rottman, and W. F. Saam, Phys. Rev. B **30**, 6549 (1984).
[33] A. F. Andreev, Zh. Eksp. Teor. Fiz. **80**, 2042 (1981).
[34] L. E. Shilkrot and D. J. Srolovitz, Phys. Rev. B **53**, 11120 (1996).
[35] M. Nowicki, C. Bombis, A. Emundts, H. P. Bonzel, and P. Wynblatt, Europhys. Lett. **59**, 239 (2002).
[36] M. Nowicki, C. Bombis, A. Emundts, H. P. Bonzel, and P. Wynblatt, New J. Phys. **4**, 60 (2002).
[37] K. Arenhold, S. Surnev, H. P. Bonzel, and P. Wynblatt, Surf. Sci. **424**, 271 (1999).
[38] A. Emundts, M. Nowicki, and H. P. Bonzel, Surf. Sci. **496**, L35 (2002).
[39] M. Methfessel, D. Hennig, and M. Scheffler, Phys. Rev. B **46**, 4816 (1992).
[40] M. Methfessel, D. Hennig, and M. Scheffler, Appl. Phys. A: Solids Surf. **55**, 442 (1992).
[41] M. McLean, Acta Metall. **19**, 387 (1971).
[42] H. P. Bonzel, Surf. Sci. **328**, L571 (1995).
[43] H. P. Bonzel (unpublished).
[44] J. L. F. Da Silva, C. Barreteau, K. Schroeder, and S. Blügel, Phys. Rev. B **73**, 125402 (2005).
[45] I. N. Stranski, Discuss. Faraday Soc. **5**, 13 (1949).
[46] J. Friedel, B. D. Cullity, and C. Crussard, Acta Metall. **1**, 79 (1953).
[47] J. K. MacKenzie, A. J. W. Moore, and J. F. Nicholas, J. Phys. Chem. Solids **23**, 185 (1962).
[48] M. C. Desjonquères, D. Spanjaard, C. Barreteau, and F. Raouafi, Phys. Rev. Lett. **88**, 056104 (2002).